Accepted Manuscript

Design, synthesis, SAR discussion, in vitro and in vivo evaluation of novel selective EGFR modulator to inhibit L858R/T790M double mutants

Haoyang Zhang, Wenkui Wu, Chao Feng, Zhaogang Liu, Enhe Bai, Xueyuan Wang, Meng Lei, Hao Cheng, Huayun Feng, Jingmiao Shi, Jia Wang, Zhao Zhang, Tao Jin, Shanshan Chen, Shihe Hu, Yongqiang Zhu

PII: S0223-5234(17)30300-8

DOI: 10.1016/j.ejmech.2017.04.036

Reference: EJMECH 9385

To appear in: *European Journal of Medicinal Chemistry*

Received Date: 26 January 2017

Revised Date: 11 April 2017

Accepted Date: 13 April 2017

Please cite this article as: H. Zhang, W. Wu, C. Feng, Z. Liu, E. Bai, X. Wang, M. Lei, H. Cheng, H. Feng, J. Shi, J. Wang, Z. Zhang, T. Jin, S. Chen, S. Hu, Y. Zhu, Design, synthesis, SAR discussion, in vitro and in vivo evaluation of novel selective EGFR modulator to inhibit L858R/T790M double mutants, *European Journal of Medicinal Chemistry* (2017), doi: 10.1016/j.ejmech.2017.04.036.

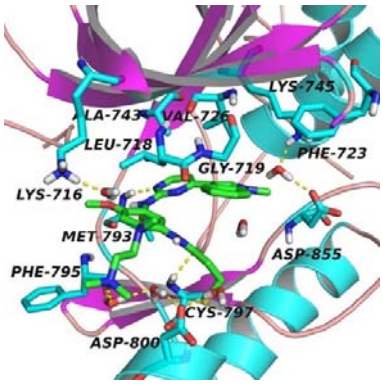

Binding of AZD9291 with T790M

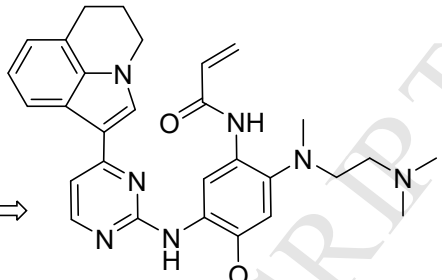

Compound 8

$EGFR^{WT}$ IC_{50}: 21.6 nM

$EGFR^{T790M/L858R}$ IC_{50}: 2.6 nM

$T_{1/2}$= 4.1 h, F%= 52.4%

hERG IC_{50}: 8.46 μM

Design, synthesis, SAR discussion, in vitro and in vivo evaluation of novel selective EGFR modulator to inhibit L858R/T790M double mutants

Haoyang Zhang,[#,†] Wenkui Wu,[#,†] Chao Feng,[‡] Zhaogang Liu,[‡] Enhe Bai,[§] Xueyuan Wang,[†] Meng Lei,[§] Hao Cheng,[‡] Huayun Feng,[§] Jingmiao Shi,[‡] Jia Wang,[‡] Zhao Zhang,[†] Tao Jin,[†] Shanshan Chen,[‡] Shihe Hu,[,‡] Yongqiang Zhu[*,†]*

[†]College of Life Science, Nanjing Normal University, No. 1 Wenyuan Road, Nanjing 210046, PR China, [‡]Jiangsu Chia Tai Fenghai Pharmaceutical Co. Ltd., No. 9 Weidi Road, Nanjing 210046, PR China and [§]College of Science, Nanjing Forestry University, No. 159 Longpan Road, Nanjing 210037, PR China

Corresponding Authors

**Prof. Yongqiang Zhu*

Phone: 86-25-85891591; Fax: 86-25-85891591; E-mail: zhyqscu@hotmail.com.

**Dr. Shihe Hu*

Phone: 86-25-57033246-8280; Fax: 86-25-57033246-8280; E-mail: hsh.2@163.com.

Author Contributions

[#]These authors contributed equally to the work.

ABSTRACT: *Based upon the modeling binding mode of marketed* **AZD9291** *with T790M, a series of 5,6-dihydro-4H-pyrrolo[3,2,1-ij]quinoline derivatives were designed and synthesized with the purpose to overcome the drug resistance resulted from T790M/L858R double mutations. The most potent compound* **8** *showed excellent enzyme inhibitory activities and selectivity with sub nanomolar* IC_{50} *values for both the single L858R and double T790M/L858R mutant EGFRs, and was more than 8-fold selective for wild type EGFR. Compound* **8** *exhibited good microsomes stabilities and pharmacokinetic properties and lower binding affinity to hERG ion channel than* **AZD9291** *and displayed strong antiproliferative activity against the H1975 non-small cell lung cancer (NSCLC) cells bearing T790M/L858R and in vivo anticancer efficacy in a human NSCLC (H1975) xenograft mouse model.*

KEYWORDS: *Non-small cell lung cancer, 5,6-Dihydro-4H-pyrrolo[3,2,1-ij]quinoline derivatives, EGFR modulator, L858R/T790M double mutants*

1. Introduction

The ErbB family of receptor tyrosine kinases plays a crucial regulatory role associated with malignancies, making this protein family an anticancer target [1]. *Epidermal growth factor receptor (EGFR) belongs to the ErbB family and is a key mediator in cellular signaling related to cell growth, proliferation, survival, and migration* [2-4]. *Overexpression or mutation of EGFR is a common feature in many human solid malignancies, especially in non-small cell lung cancer (NSCLC)* [5-7]. *Therefore, EGFR represents a valuable target for the design of anticancer agents* [8-11]. *The first-generation EGFR inhibitors* **erlotinib** *and* **gefitinib** *(Fig. 1) have been used in clinic for the treatment of EGFR-mutated NSCLC (such as L858R and delE746-A750)* [12, 13]. *Unfortunately, the clinical efficacies of* **erlotinib** *and* **gefitinib** *were limited by the acquired drug resistance, such as that induced by the mutation of the gatekeeper residue*

(T790M) which was detected in 50% of clinically acquired drug resistant patients [14, 15]. *This mutation decreases the binding of ATP-competitive inhibitors to the kinase and restores ATP affinity to EGFR* [16].

In order to overcome drug resistance induced by T790M, the second-generation irreversible inhibitors had been developed including **afatinib** *and* **dacomitinib** *(Fig. 1). These inhibitors contained electrophilic Michael-acceptor moieties that could covalently modify the conserved cysteine residue (Cys797) at the lip of the ATP binding cleft of EGFR* [17-19]. *However, their clinical efficacy had been limited by associated skin rash and gastrointestinal toxicity because of their poor kinase selectivity between EGFR T790M mutants and the wild-type (WT) EGFR* [20].

The desire to improve the selectivity of EGFR T790M over the WT EGFR led to the third-generation of irreversible EGFR inhibitors. Since the discovery of **WZ-4002**, *a number of , -unsaturated vinyl amide inhibitors entered clinical trials, such as* **CO-1686**, **PF-06459988** *and* **AZD9291** *(Fig. 1)* [21-24]. *Among them,* **AZD9291** *which had an amino pyrimidine scaffold, showed 200-fold selectivity for T790M/L858R double mutants over WT EGFR* [25] *and was approved for the treatment of NSCLC patients with EGFR T790M mutation by FDA in November 2015.*

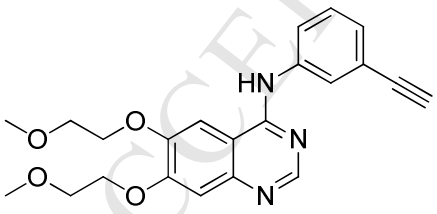

erlotinib

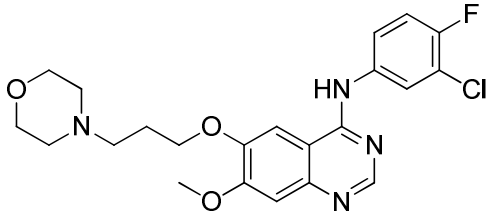

gefitinib

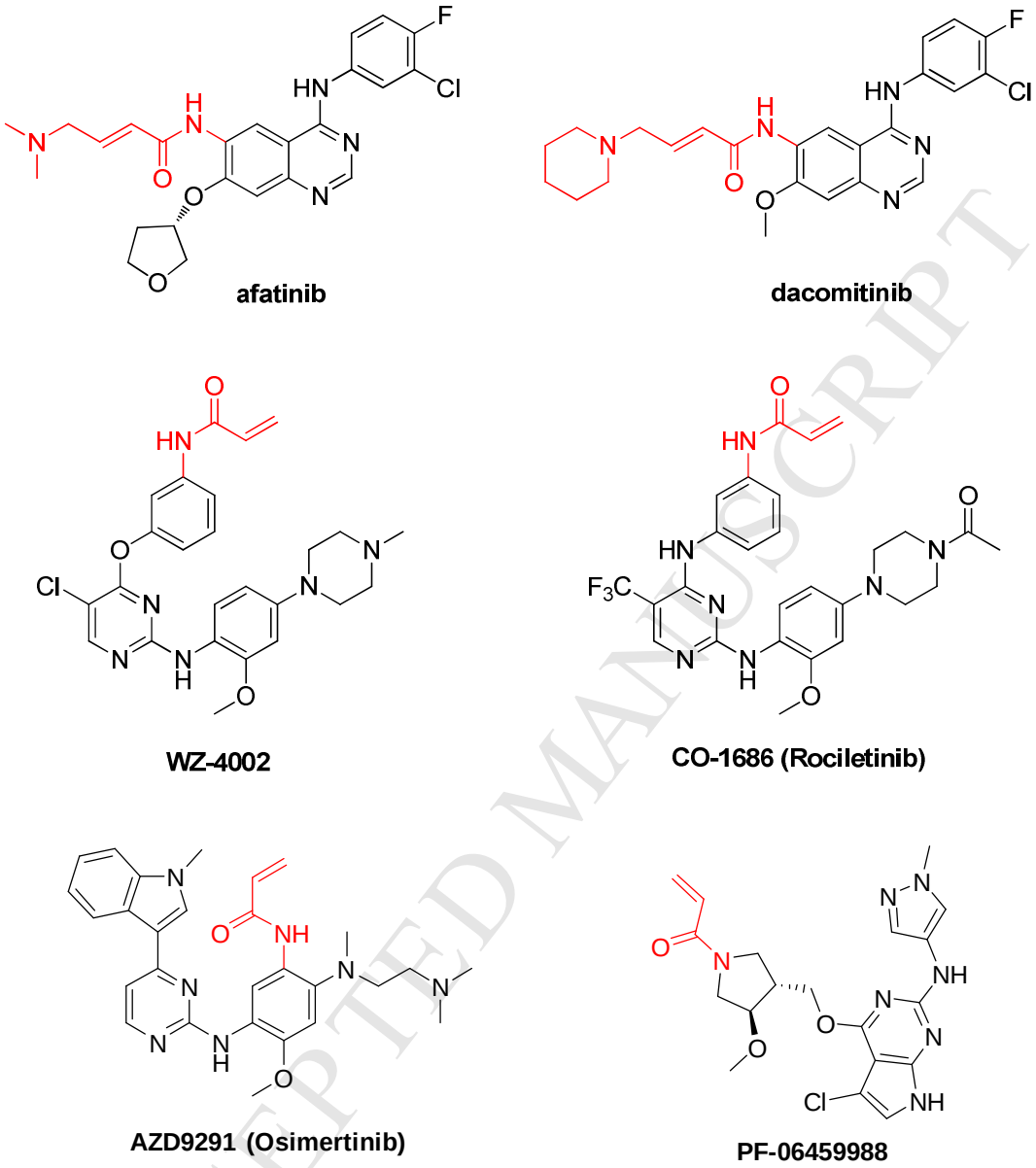

Fig. 1. *Structures of different generation EGFR inhibitors.*

AZD9291 *had been reported to have a few common adverse events in clinical trials, such as diarrhea, rash and decreased appetite. And the morbidity of diarrhea, rash and cardiotoxicity increased with escalating doses of* **AZD9291** [26]. *To overcome the drawbacks of* **AZD9291**, *in this manuscript, we described the design, synthesis, in vitro and in vivo biological evaluation of a series of novel selective T790M inhibitors.*

2. Results and discussion

2.1. Chemistry

The synthetic routes of target compounds **6-16** *and* **22-30** *were outlined in Schemes 1 and 2, respectively. For the preparation of compounds* **6−12** *(Scheme 1), commercially available 2- or 5-substituted pyrimidines* **1** *were firstly coupled with 1-methyl-1H-indole or 5,6-dihydro-4H-pyrrolo[3,2,1-ij]quinolone fragments to give intermediates* **2** *(***2a** *or* **2b***) in moderate to high yields (45.0-90.0%) with the catalyst aluminum chloride. And then the 6-chloro groups of* **2** *were substituted by 4-fluoro-2-methoxy-5-nitroaniline moiety to give the intermediates* **3** *with the yields of 81.5-92.0%. The fluoro groups of* **3** *were substituted by the N,N,N-trimethylethane-1,2-diamine to produce intermediates* **4** *with the yields of 60.0-78.0%. Subsequent reduction of the nitro groups of* **4** *with hydrogen gave amines* **5**, *which were not purified and directly used in the next reaction. After acylation of amines* **5** *with acryloyl chloride and elimination of hydrochloride with sodium hydroxide, the desired final molecules* **6-12** *were obtained with the yields of 25.0-65.5%.*

Scheme 1. *Synthetic Route for Target Compounds* **6-12**[a]

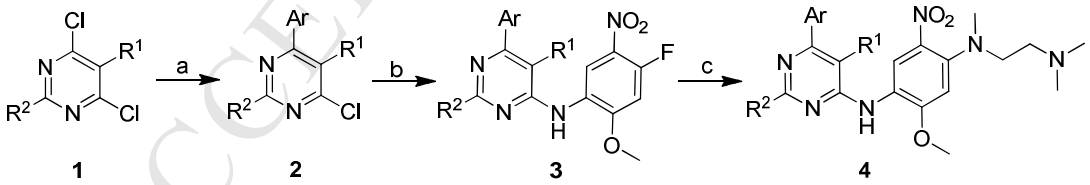

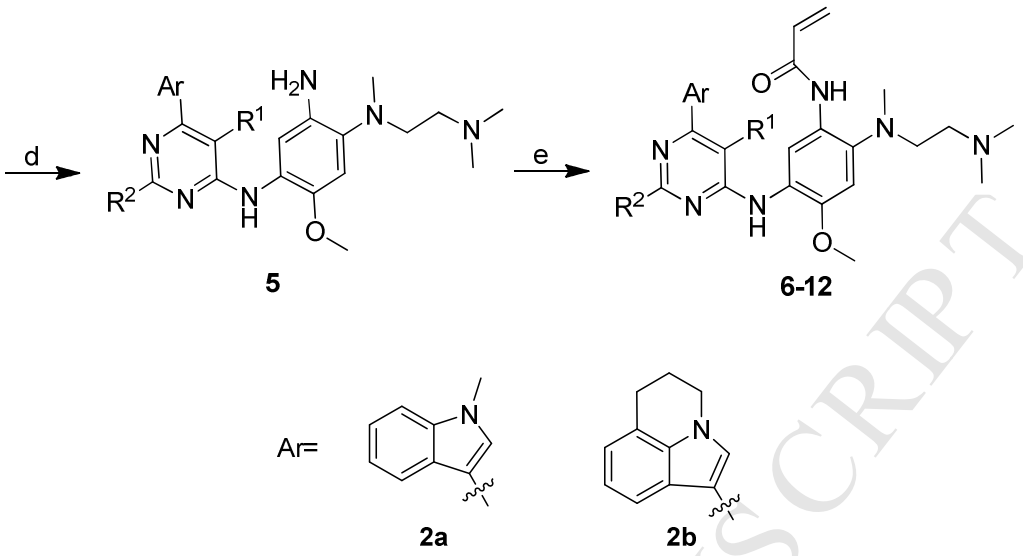

[a]*Reagents and conditions: (a) 1-methyl-1H-indole (1 equiv) or 5,6-dihydro-4H-pyrrolo [3,2,1-ij]quinolone (1 equiv), $AlCl_3$ (1 equiv), 1,2-dimethoxyethane (DME), 85 °C, 6 h, 45.0-90.0%; (b) 4-fluoro-2methoxy-5-nitroaniline (1.1 equiv), tosic acid monohydrate (1.1 equiv), 1,4-dioxane, 90 °C, 9 h, 81.5-92.0%; (c) N,N,N'-trimethylethane-1,2-diamine (1.1 equiv), N,N-diisopropylethyl- amine (DIPEA) (1.5 equiv), N,N-dimethylacetamide (DMAC), 140 °C, 6 h, 60.0-78.0%; (d) 10% Pd/C (0.2 equiv), H_2, MeOH, rt, overnight; (e) 3-chloropropanoyl chloride (1 equiv), NaOH (4 equiv), THF, rt-65 °C, overnight, 25.0-65.5%.*

The target compounds **13-16** *and* **22−30** *were prepared from commercially available 2,4-dichloro pyrimidine* **17**. *Firstly 4-chloro of starting material* **17** *was substituted by 3-methyl-1H-indole and 1H-indazole groups to give the key intermediates* **18a** *and* **18b** *with the yields of 86.4% and 80.0%, respectively. For the preparation of intermediate* **18c**, *4-chloro group of starting material* **17** *was substituted by 5,6-dihydro-4H-pyrrolo[3,2,1-ij]quinolone with the catalyst aluminum chloride in high yield (90.1%). Then the 2-chloro groups of compounds* **18** *were substituted by 4-fluoro-2-methoxy-5-nitroaniline to give the intermediates* **19** *(yields 84.0-95.0%). The fluoro groups of* **19** *were substituted by different amines R to produce intermediates*

20 *with moderate to high yields (60.5-80.0%). Subsequent reduction of the nitro groups of* **20** *with hydrogen gave amines* **21**, *which were not purified and directly used in the next reaction. After acylation of* **21** *with acryloyl chloride and elimination of hydrochloride with sodium hydroxide, the desired compounds* **13-16** *and* **22-30** *were obtained with the yields of 24.9-70.0%.*

Scheme 2. *Synthetic Route for Target Compounds* **13-16** *and* **22-30**[a]

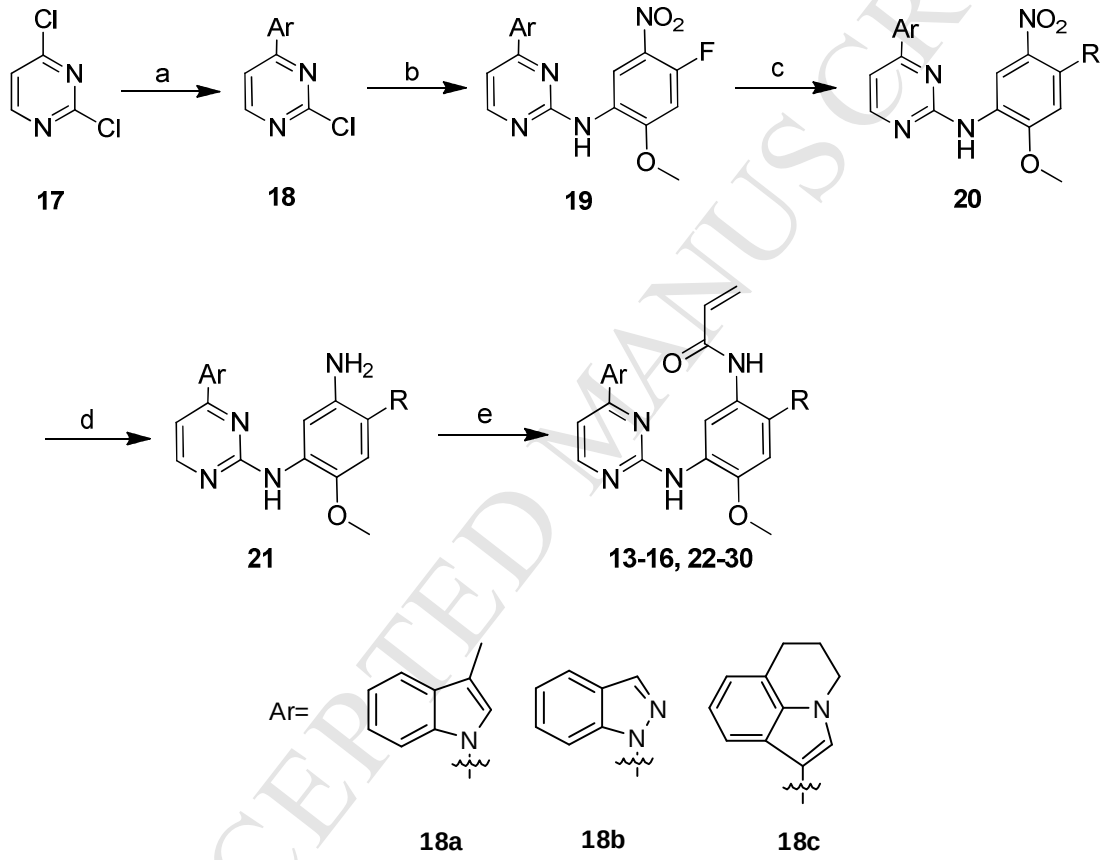

[a]*Reagents and conditions: (a) 3-methyl-1H-indole (1 equiv) or 1H-indazole (1 equiv),* K_2CO_3 *(2 equiv),* MeCN, reflux, overnight, *80.0-86.4%; 5,6-dihydro-4H-pyrrolo[3,2,1-ij]quinolone (1 equiv),* $AlCl_3$ *(1 equiv), DME, 80 °C, 6 h, 90.1%; (b) 4-fluoro-2-methoxy-5-nitroaniline (1.1 equiv), tosic acid monohydrate (1.1 equiv), 1,4-dioxane, 85 °C, 8 h, 84.0-95.0%; (c) different substituted amines R (1.1 equiv), DIPEA (1.5 equiv), DMAC, 140 °C, 6 h, 60.5-80.0%; (d) 10%*

Pd/C (0.2 equiv), H_2, MeOH, rt, overnight; (e) acryloyl chloride (1 equiv), DIPEA (2.0 equiv), CH_2Cl_2, -10 °C, 0.5 h, 24.9-70.0%.

2.2. Design strategy of the new compounds

Without the crystal complex of **AZD9291** *binding to the T790M EGFR kinase domain, we employed a published T790M structure (PDB code: 3IKA) to model the binding mode with* **AZD9291** *(Figs. 2 and 3). The docking mode indicated that* **AZD9291** *bound to the outer edge of the ATP-binding pocket. The pyrimidine core of the molecule formed two hydrogen bonds with Met793 residue in the kinase hinge: one with the indole group adjacent to the gatekeeper residue, and the other with the dimethylamine moiety positioned in the solvent channel, while Cys797 covalently bonded to the acrylamide group* [22]. *Furthermore, several vander Waals interactions existed between* **AZD9291** *and the residues of protein, such as the pyrimidine ring with Ala743, and the indole ring with Val726 and Phe723, respectively (Fig. 3)* [27]. *These interactions were envisioned to be important for improving the activity and selectivity against mutated EGFR kinase* [28].

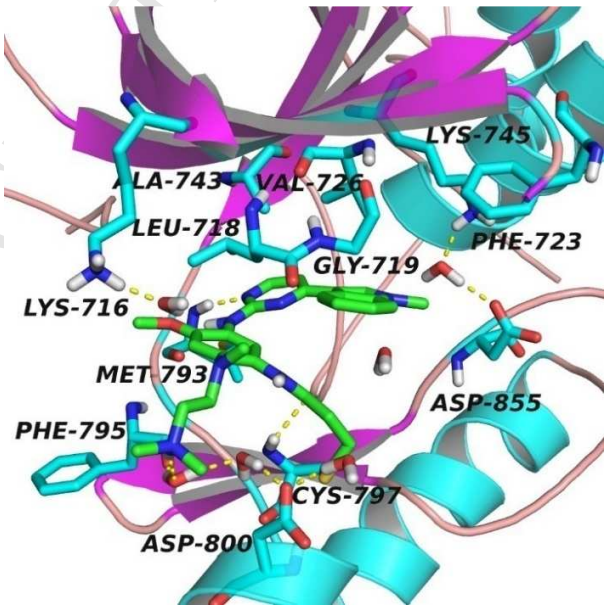

Fig. 2. Docking pose of **AZD9291** in the complex of EGFR T790M mutant.

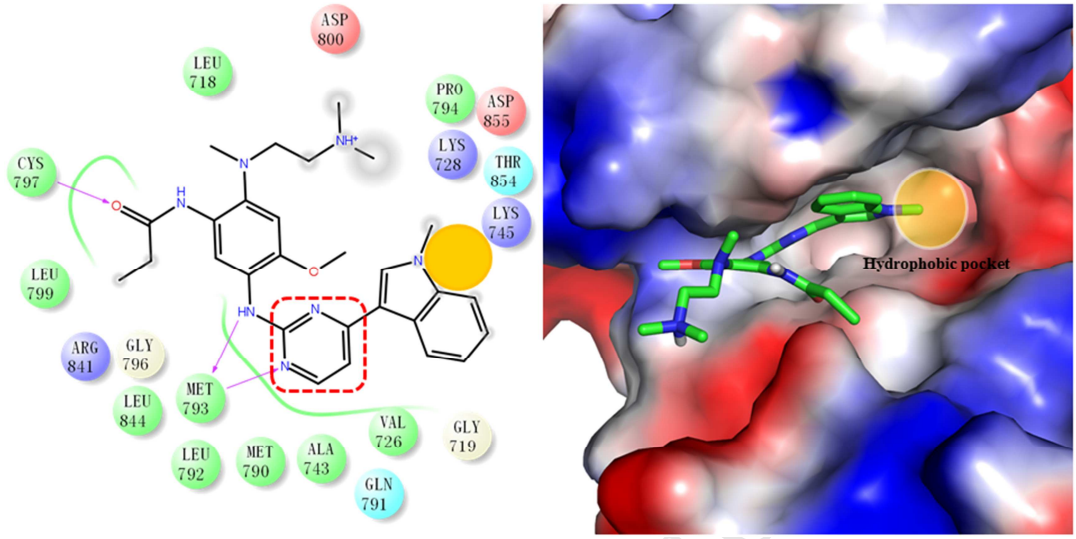

Fig. 3. Interaction map of **AZD9291** with the EGFR T790M mutant and the overview in the binding site.

Based upon the binding mode of **AZD9291** *with T790M active domain, we modified the substitution position of the pyrimidine ring and expanded the indole ring (Fig. 4) to increase the binding interaction and selectivity of the inhibitors with T790M EGFR kinase, which may reduce their affinity for the human ether-a-go-go related gene (hERG) channel (cardiotoxicity). And a number of side chain amines (R) were also modified with the purpose to improve the potency and physical properties of the inhibitors.*

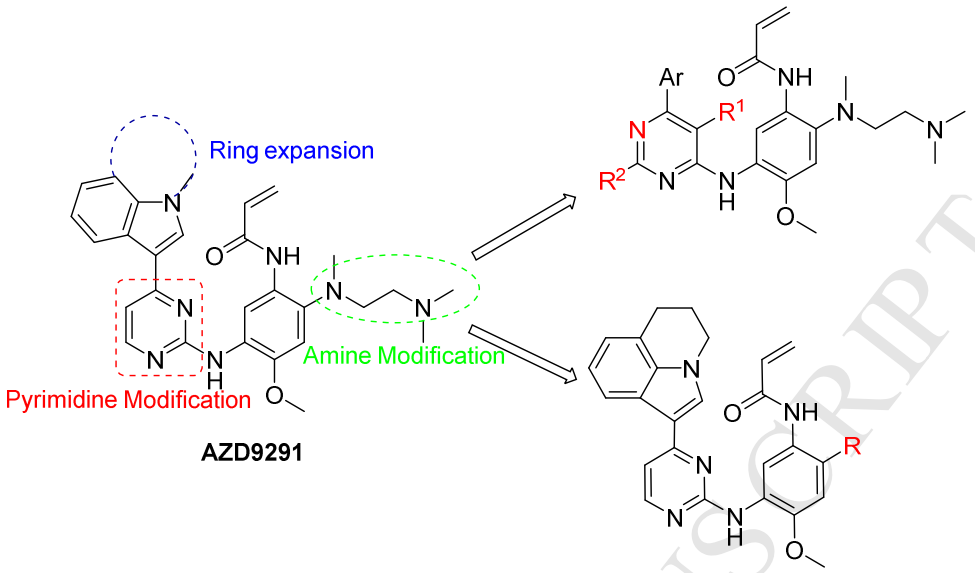

Fig. 4. Design strategy of the new compounds based on **AZD9291**.

2.3. Biological evaluation

According to our design strategy (Fig. 4), a series of novel T790M inhibitors with 2- and 4-amino pyrimidine scaffold were designed and synthesized (Table 1). The kinase inhibitory activities of the target compounds were evaluated via a well-established FRET-based Z'-Lyte assay [29] *against different types of EGFR kinases (Table 1).*

Compared with 2-amino pyrimidine standard **AZD9291**, *most of 4-amino pyrimidine analogues* **12-16** *showed greatly decreased activities against wild type (WT) EGFR, single mutant L858R and double mutant T790M/L858R (TL), but compounds* **10** *and* **11** *displayed strong activities against all of these three EGFRs (all* IC_{50} *values were less than 5 nM). However, these two compounds showed less selectivity between WT and TL EGFR (the ratio of WT/TL was 1.4 and 1.2, respectively). Screening of 2- and 4-amino substituted pyrimidine cores indicated that the former could be selected as the template to develop. The biological results demonstrated that ring expansion of indole moiety dramatically affected the activities and selectivity for the 2-amino substituted pyrimidine analogues. Introduction of 5,6-dihydro-4H-*

pyrrolo[3,2,1-ij]quinolone group at the indole position led to the same activity and selectivity as the standard **AZD9291**. *For example, compound* **8** *inhibited the wild type EGFR, single mutant L858R and double mutants T790M/L858R (TL) with the* IC_{50} *values of 21.6, 6.0 and 2.6 nM, respectively and the corresponding* IC_{50} *values of* **AZD9291** *were 19.7, 6.0 and 2.1 nM, respectively, which suggested that the spatial position of indole group in* **AZD9291** *close to the gatekeeper residue would be large enough for the ternary ring structure group such as 5,6-dihydro-4H-pyrrolo[3,2,1-ij]quinoline moiety. However, the substitution of 1-methyl-1H-indole (***AZD9291***) with 3-methyl-1H-indole (compound* **6***) dramatically decreased the activity and selectivity (Table 1). Furthermore, the introduction of 1H-indazole (compound* **7***) moiety led to complete loss of activities against all of the three EGFR kinases. For the 4-amino compound, modification of indole position did not change the activity and selectivity in a large extent. For example, both 1-methyl-1H-indole (compound* **10***) and 5,6-dihydro-4H-pyrrolo[3,2,1-ij]quinolone (compound* **11***) moieties led to the same activities against WT, L858R and TL kinases (all* IC_{50} *values were less than 5 nM) and the similar selectivity. The same results could be concluded for 1-methyl-1H-indole substituted compound* **12** *and 5,6-dihydro-4H-pyrrolo[3,2,1-ij]- quinolone substituted compound* **16**. *Different substitutes at* R^1 *and* R^2 *positions affected the activities and selectivity of both 2- and 4-amino pyrimidine analogues. For 2-amino substituted compounds, the substitution of hydrogen at* R^2 *position (***AZD9291***) with methoxy group (compound* **9***) decreased the TL activity (*IC_{50}*: 13.0 nM vs 2.0 nM) with 6.5 folds, but the selectivity was increased with 5.3 folds (WT/TL: 52.6 vs 9.9). For 4-amino substituted compounds, substitution of the hydrogen at* R^1 *position (compound* **10**, IC_{50}*: 1.6 nM) with fluoro (compound* **13**, IC_{50}*: 94.8 nM) and methoxy groups (compound* **14**, IC_{50}*: 212.5 nM) dramatically decreased the TL activities. Different groups at* R^2 *position also had great influence on the activity and selectivity. Methyl and methoxy groups at* R^2 *position decreased the TL activities*

and increased the selectivity in a certain extent. Compared with compound **10**, *methoxy substituted compound* **16** *was 6-fold less potent in activity, but its selectivity was increased by more than 40 folds, while the methyl substituted compound* **15** *was 37-fold less potent in activity, but the selectivity was increased in only 2 folds. Based on the activities and selectivity, compound* **8** *was selected as a lead to optimize.*

Table 1. *Enzymatic Inhibitory Activities of Compounds* **6-16** *and* **AZD9291**[a]

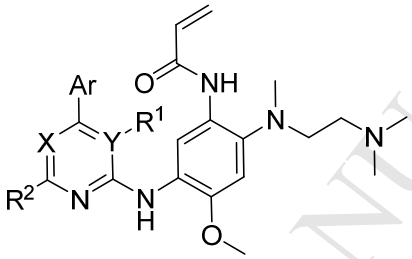

Compd.	R^1	R^2	Ar	X	Y	IC_{50} (nM)[a]			Selectivity
						WT[b]	L858R	TL[c]	(WT/TL)
6	-	H	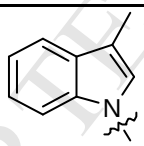	C	N	714.5	185.6	287.4	2.5
7	-	H	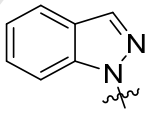	C	N	NA[d]	>600	>600	-
8	-	H	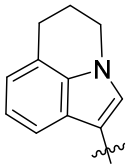	C	N	21.6	6.0	2.6	8.3

9	-	OMe	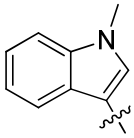	C	N	685.0	154.6	13.0	52.6
10	H	H	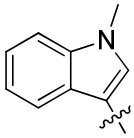	N	C	2.3	2.2	1.6	1.4
11	H	H	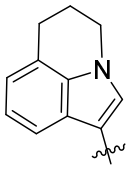	N	C	3.1	1.2	2.6	1.2
12	H	OMe	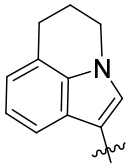	N	C	543.0	181.1	22.0	24.7
13	F	H	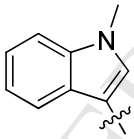	N	C	32.1	9.9	94.8	0.34
14	OMe	H	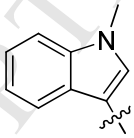	N	C	222.5	55.5	212.5	1.0
15	H	CH_3	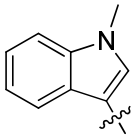	N	C	192.0	46.5	60.6	3.2
16	H	OMe	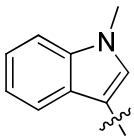	N	C	636.0	123.4	10.9	58.3

AZD9291	-	H	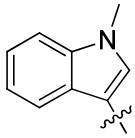	C	N	19.7	6.1	2.0	9.9

[a]Enzymatic inhibitory-activity assays were performed using the FRET-based Z′-Lyte assay. All experiments were repeated at least three times. [b]WT, wild type EGFR. [c]TL, T790M/L858R double mutants. [d]NA, not active.

After the optimization of ring expansion and pyrimidine moiety, the modification of amine R groups was carried out. Different amine moieties were screened and the results were showed in Table 2. Firstly, the terminal N atom (compound **8***) was changed to its isostere O atom (compound* **22***) to investigate the activity and selectivity by application of the bioisosterism method. The results indicated that the activities of compound* **22** *against three kinds of kinases were dramatically decreased although the selectivity was 3-fold higher than that of compound* **8**. *Then the effect of the amidation of terminal tertiary N was evaluated. Amides* **23** *and* **24** *were inactive in the inhibition of WT kinase and only showed micromole level against L858R and TL kinases, which may be due to the loss of hydrogen donor after amidation of terminal N atom. Then the effect of different substituents of N atom linked to the core was investigated. After cyclization with four membered ring (compound* **25***), the activities against L858R and TL kinases nearly decreased 2 folds compared with compound* **8**. *When the distance of two nitrogen atoms of R group was increased, the activities against three kinases were all decreased. For example, compounds* **26** *and* **27** *lost the potencies against all forms of the EGFR kinases compared with compound* **8.** *Compound* **28,** *which was cyclized with five membered ring, remained the potencies against EGFR kinases, but the selectivity slightly reduced. When the amine moiety R was replaced with piperazine moiety (compound* **29***), all the inhibitory activities reduced significantly and compound* **30** *was inactive in the inhibition of all forms of the EGFR kinases after amidation*

of piperazine ring. The optimized results illustrated that the R position might be N,N,N-trimethylethane-1,2-diamine group to maintain the stronger inhibition against EGFR kinases and the better selectivity.

Table 2. *Enzymatic Inhibitory Activities of* **22-30** *and* **AZD9291**[a]

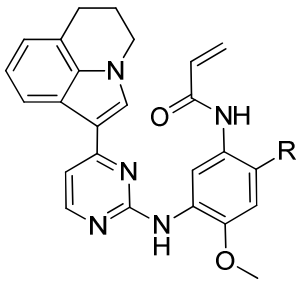

Compd.	R	IC_{50} (nM)[a]			Selectivity
		WT[b]	L858R	TL[c]	(TL/WT)
8	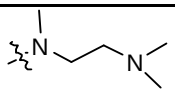	21.6	5.3	2.9	7.4
22	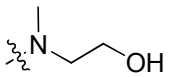	838.5	192.3	34.8	24.1
23	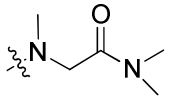	>1000	498.0	278.2	>3.6
24	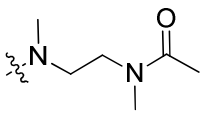	>1000	385.5	188.2	>5.3
25	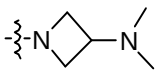	63.9	13.6	4.9	13.0

26	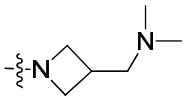	202.1	11.6	6.7	30.2
27	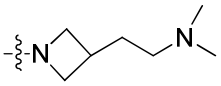	251.1	14.5	11.8	21.3
28	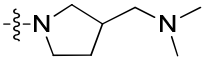	8.8	4.0	1.9	4.6
29	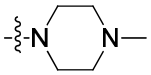	877.4	64.3	55.5	15.8
30	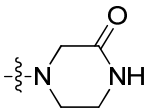	NA[d]	427.7	1230.0	-
AZD9291		13.8	4.2	1.9	7.2

[a]Enzymatic inhibitory-activity assays were performed using the FRET-based Z′-Lyte assay. All experiments were repeated at least three times. [b]WT, wild type EGFR. [c]TL, T790M/L858R double mutants. [d]NA, not active.

The antiproliferative effects of the new potential inhibitors with the IC_{50} values of enzymatic inhibition less than 10 nM were further investigated to evaluate their potential antitumor activities in cancer cell lines (Table 3). The results displayed that compounds **10**, **11** *and* **28** *were active against A431, HCC827 and H1975 NSCLC cells harboring wild-type EGFR, EGFR delE746-A750 and EGFR L858R/T790M, respectively. But these compounds showed less selectivity between wild-type and mutant cell lines. Compounds* **8**, **9**, **12**, **16**, **25** *and* **26** *were nearly inactive in the inhibition of wild-type A431 cell and much active against mutant cell lines*

and showed high selectivity. The SAR analysis of these compounds indicated that after cyclization with four membered ring (compounds **25** *and* **26***) of amine R groups, the selectivity against HCC827 and H1975 cancer cells nearly remained compared with compound* **8***, but the activities decreased slightly. Interestingly, introduction of a methoxy group in the 6-position of the 2-aminopyrimidine ring (compound* **9***) and the 2-position of the 4-aminopyrimidine rings (compounds* **12** *and* **16***) led to a significant loss in potencies against the cancer cells. So based on the selectivity and activity data against the mutant cancer cell lines, compound* **8** *were selected to be further evaluated the drug availability.*

Table 3. *Cell Viabilities of Representative Compounds*[a]

	NSCLC cell lines IC_{50} (nM)			Selectivity
Compd.	A431 (WT[b])	HCC827 (del E746-A750)	H1975 (TL[c])	(TL/WT)
8	869.8	109.2	102.6	8.5
9	>10000	1166.0	319.9	>31.3
10	128.4	16.2	33.8	3.8
11	121.7	24.3	37.8	3.2
12	>10000	1207.0	563.0	>17.8
16	>10000	925.0	210.2	>47.6
25	1123.0	98.2	143.3	7.8
26	1468.0	289.7	166.2	8.8
28	514.2	71.7	99.9	5.1

AZD9291	615.6	61.6	67.0	9.2

[a] *All experiments were repeated at least three times.* [b]*WT, wild type EGFR.* [c]*TL, T790M/L858R double mutant.*

The metabolic stability of the promising compound **8** *was determined with various species of liver microsomes, such as human, mouse, rat, dog and monkey liver microsomes (Data were shown in Table 4). And the marketed* **AZD9291** *was selected as the standard. The half-life ($T_{1/2}$) and intrinsic clearance (CL_{int}) parameters were used to evaluate their metabolic stabilities. It could give a good indication of the in vivo hepatic clearance when the overall clearance mechanism was metabolic and when oxidative metabolism dominates (i.e., $CL_{metabolic} \gg CL_{renal} + CL_{biliary} + CL_{other}$)* [30, 31]. *Table 4 revealed that compound* **8** *displayed good metabolic stabilities. The half-life of* **8** *in human liver microsome were more than 180 minutes, which showed that it almost was not metabolized by human liver microsome and the control* **AZD9291** *showed similar result. For other species, mouse liver microsome metabolized compound* **8** *in 11.9 minutes, which was more rapidly than other microsomes. Furthermore, compound* **8** *was metabolized in shorter time than* **AZD9291** *in mouse, rat and monkey liver microsomes except dog. So this compound could be metabolized more rapidly than* **AZD9291** *after binding with target and showed less toxicity than* **AZD9291**, *which was displayed during our in vivo experiments.*

Table 4. *Stabilities of Compounds* **8** *and* **AZD9291** *in Liver Microsomes of Various Species*

	8		**AZD9291**	
Liver microsomes	$T_{1/2}$	CL_{int}	$T_{1/2}$	CL_{int}

	(min)	(mL/min/kg)	(min)	(mL/min/kg)
Human	>180	ND[a]	ND[a]	ND[a]
Mouse	11.9	456.8	23.9	228.4
Rat	46.2	54.0	62.4	40.0
Dog	31.5	63.4	21.0	95.0
Monkey	28.9	64.8	63.0	29.7

[a]*ND: not detected.*

Furthermore, data of the metabolic stabilities in human and rat hepatocytes for compound **8** *and* **AZD9291** *showed the similar results as that of microsome stabilities (Data were shown in Table 5). Compound* **8** *was metabolized more rapidly than* **AZD9291** *in both human and rat hepatocytes. And the metabolic degradation of compound* **8** *in human hepatocytes was slower than rat one, which was consistent with the results of liver microsomes stabilities.*

Table 5. *Stabilities of Compounds* **8** *and* **AZD9291** *in Hepatocyte*

	8		**AZD9291**	
Hepatocyte	$T_{1/2}$ (min)	CL_{int} (μL/min/10^6 cell)	$T_{1/2}$ (min)	CL_{int} (μL/min/10^6 cell)

Human	138.6	5.0	>180	ND[a]
Rat	33.0	21.0	57.8	12.0

[a]*ND: not detected.*

With these encouraging in vitro data, candidate **8** *was further investigated by profiling po and iv pharmacokinetics in male Sprague-Dawley (SD) rats. The results were illustrated in Table 6. After oral administration in male SD rats, compound* **8** *showed longer half life time than* **AZD9291** *($T_{1/2}$: 4.1 vs 3.8 h), partially because of its lower systemic clearance (CL: 5169.7 vs 6600.0 (mL/h)/kg). Furthermore, good exposure was observed for compound* **8** *($AUC_{0\text{-}inf}$: 1021.0 h·ng/mL). It also showed a good oral bioavailability (52.4%), approximately equal to* **AZD9291** *in our test (66.5%).*

Table 6. *In Vivo Pharmacokinetic Parameters for Compounds* **8** *and* **AZD9291**[a]

Parameters	**8**		**AZD9291**	
Dose (mg/kg)	10.0 (po)	1.0 (iv)	10.0 (po)	1.0 (iv)
$T_{1/2}$(h)	4.1	4.5	3.8	4.5
T_{max}(h)	3.3	-	2.7	-
C_{max}(ng/mL)	111.0	-	111.0	-
$AUC_{0\text{-}t}$(h·ng/mL)	994.7	189.7	937.3	141.0
$AUC_{0\text{-}inf}$(h·ng/mL)	1021.0	194.0	954.3	152.7
CL((mL/h)/kg)	-	5169.7	-	6600.0
MRT(h)	5.7	4.7	5.7	4.8

F(%)	52.4	-	66.5	-

[a]*Pharmacokinetic parameters following administration in male Sprague−Dawley rats.*

Because of its potent activity in inhibiting EGFR T790M/L858R kinases and NSCLC cell growth and good pharmacokinetic properties, compound **8** *was further evaluated for in vivo antitumor efficacy using an EGFR L858R/T790M-driven human NSCLC xenograft mouse model of H1975 (Table 7 and Fig.5). SCID mice bearing established H1975 tumor xenografts were dosed orally with compound* **8** *at 5, 10 and 20 mg/kg daily over an 18-day period. The results showed that the tumor volume inhibition was dose-dependent (Fig.5). Dosing at 5 mg/kg/day, the tumor volume was reduced in a certain extent compared with the control PBS and treatment with 10 mg/kg/day of compound* **8** *nearly inhibited tumor growth. When the dose was increased to 20 mg/kg/day, compound* **8** *displayed significant in vivo antitumor efficacy and induced tumor stasis. The tumor growth values (T/C%) were 56.4%, 25.7% and 12.1% at three different doses, respectively. And the tumor growth inhibition values (TGI%) were 46.8%, 83.5% and 96.3%, respectively (Table 7). In addition, compound* **8** *was well-tolerated and no mortality or significant loss of body weight was observed during treatment at all doses.*

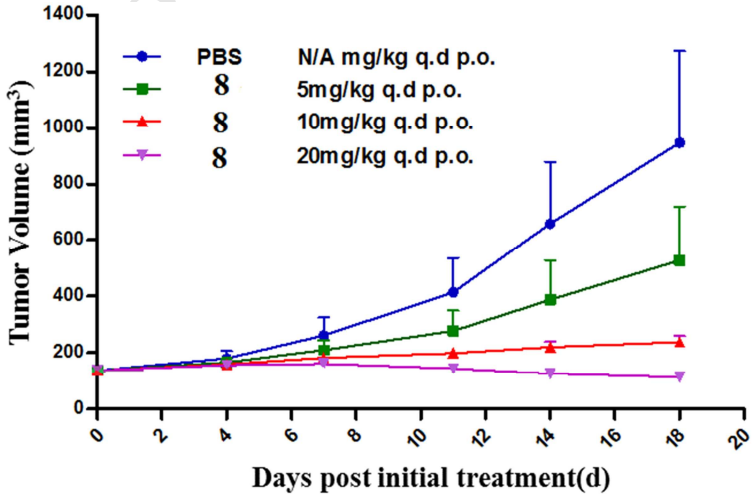

Fig. 5. *In vivo activity of* **8** *in the human NSCLC (H1975) xenograft nude mouse model.*

Table 7. *In Vivo Antitumor Effect of* **8** *in Human H1975 Xenograft Nude Mouse Model*

Group	TV[a] Mean (mm^3)	RTV[b] Mean	T/C[c] (%)	RTV SF[d]	TW[e] Mean （Day18, g）	TGI[f] (%)
Control (PBS[g])	948.05	6.77			1.88	
8 (5 mg/kg)	527.78	3.82	56.4%	**	1	46.8%
8 (10 mg/kg)	239.33	1.74	25.7%	**	0.31	83.5%
8 (20 mg/kg)	113.52	0.82	12.1%	**	0.07	96.3%

*[a]TV: tumor volume; [b]RTV: relative tumor volume, the individual RTV was calculated as follows: RTV = V_t/V_0, where V_t is the volume on each day of measurement, and V_0 is the volume on the day of initial treatment; [c]T/C(%)=$RTV_{treatment}/RTV_{control}\times 100\%$; [d]SF: statistical significance (*p<0.05, **p<0.01); [e]TW: tumor weight, [f]TGI: tumor growth inhibition, TGI(%)= ($TW_{control}$-$TW_{treatment}$) /$TW_{control}\times 100\%$; [g]PBS: phosphate buffer saline.*

The human ether-a-go-go related gene (hERG) ion channel inhibition, which may result in a concomitant risk of sudden death, must be avoided during drug development [32]. *The inhibition of the hERG channel by compounds* **8** *and* **AZD9291** *was evaluated in HEK293 cells using an in vitro Ion Works Quattro study* [33]. *Fig. 6 highlighted the observation that compound* **8** *showed 14.8-fold lower affinities for the hERG ion channel than* **AZD9291**. *This result suggested that compound* **8** *may have the less probability to induce QT interval prolongation than* **AZD9291** *for the patients.*

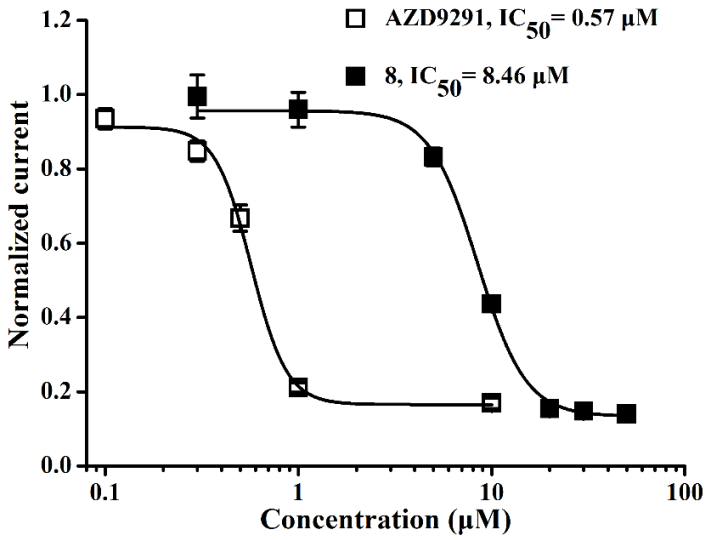

Fig. 6. *hERG current inhibition of compounds* **8** *and* **AZD9291**.

3. Conclusion

A novel series of selective covalent EGFR T790M inhibitors were designed and synthesized based on the modeling binding mode of marketed drug **AZD9291** *with EGFR T790M mutant. The structure-activity relationship (SAR) was discussed in detail and the results demonstrated that substitution with 5,6-dihydro-4H-pyrrolo-[3,2,1-ij] quinolone moiety at the para-position of 2-aminopyrimidine was considered as a novel strategy for maintaining EGFR T790M inhibitory activity and selectivity. Among the most promising inhibitors, compound* **8** *potently inhibited the enzymatic function of EGFR T790M/L858R with an* IC_{50} *value of 2.6 nM and NSCLC H1975 cell with an* IC_{50} *value of 102.6 nM. In vitro and in vivo metabolic stability studies also suggested that compound* **8** *also exhibited good pharmacokinetic properties with oral bioavailability of 52.4%. Moreover, an in vivo antitumor efficacy study demonstrated that compound* **8** *significantly inhibited tumor growth in an EGFR T790M/L858R-driven human NSCLC xenograft mouse model by po dosing at 20 mg/kg/day. The lower binding affinities of compound* **8** *to the hERG ion channel than* **AZD9291** *suggested that this candidate may be less cardiotoxic than*

AZD9291. *Therefore, the in vitro and in vivo data indicated that compound* **8** *had very desirable profiles to be selected as a clinical candidate.*

4. Experimental section

4.1. Chemistry

General methods for chemistry. *Unless otherwise specified, reagents were purchased from commercial suppliers and used without further purification. Absolutely anhydrous solvents (CH_2Cl_2, THF, DMF, etc.) were purchased from Aldrich packaged under nitrogen in Sure/Seal bottles. Yields refer to chromatography unless otherwise stated. All reactions were monitored by thin-layer chromatography carried out on silica gel aluminum sheets (60F-254) and spots were visualized with UV light or iodine. All reactions involving air or moisture-sensitive reagents were performed under an argon atmosphere. ^{1}H NMR and ^{13}C NMR spectra were recorded at room temperature on BRUKER Avance 400 spectrometers. Chemical shifts were reported in parts per million (ppm, units), and tetramethylsilane (TMS) was used as an internal reference. Coupling constants (J) were expressed in Hertz. Mass spectra were obtained using Agilent LC-MS (1956B) instruments in electrospray positive and negative ionization modes. High-resolution mass spectra (HRMS) were recorded on a ZAB-HS instrument using an electrospray source (ESI). All the final products had purity of 95%. The purity of the final products was determined by UPLC (Thermo) on a Syncronis C18 column (50 mm×2.1 mm, 1.7 μm) with 0.04% TFA/ACN (gradient eluted program: 0-7 min 90/10 v/v; 7.1-10 min 0/100 v/v; 10.1-13 min 90/10 v/v) at 0.4 mL/min flow rate and 254 nm detector wavelength.*

4.1.1 *1-(2-chloropyrimidin-4-yl)-3-methyl-1H-indole (18a)*

General procedure for the synthesis of compounds **18a and 18b**. *To a solution of 2,4-dichloropyrimidine (12.49 g, 83.63 mmol) in acetonitrile (160 mL) was added 3-methyl-1H-indole (10.00 g, 76.23 mmol) and K_2CO_3 (21.07 g, 152.47 mmol) and the mixture stirred at reflux*

overnight. The reaction was cooled to room temperature, water (100 mL) was added, the mixture was extracted with dichloromethane (DCM) (3 × 100 mL), dried with Na_2SO_4, filtered and concentrated to give a tan solid (16.05 g, 86.4 % yield): ^{1}H NMR(400 MHz, DMSO-d_6) 8.65 (d, J = 5.8 Hz, 1H), 8.56 (d, J = 8.3 Hz, 1H), 7.95 (s, 1H), 7.79 (d, J = 5.9 Hz, 1H), 7.59 (d, J = 7.6 Hz, 1H), 7.38 (t, J = 7.7 Hz, 1H), 7.29 (t, J = 7.4 Hz, 1H), 2.29 (s, 3H). MS (ESI) m/z 244.2 $[M+H]^+$.

4.1.2 ***N-(4-fluoro-2-methoxy-5-nitrophenyl)-4-(3-methyl-1H-indol-1-yl)pyrimidin-2-amine (19)***

*1-(2-chloropyrimidin-4-yl)-3-methyl-1H-indole (***18a***) (20.00 g, 82.07 mmol), 4-fluoro-2-methoxy-5-nitroaniline (16.80 g, 90.28 mmol) and 4-methyl-benzenesulfonic acid monohydrate (17.17 g, 90.28 mmol) were heated at 85 °C in 1,4-dioxane (300 mL) for 8 h. The reaction was cooled to room temperature and diluted with water (200 mL) and 40% aq NaOH added until pH = 9. The solid was collected by filtration and washed with EtOH (50 mL) to afford the yellow solid (30.00 g, 92.9 % yield): ^{1}H NMR (400 MHz, DMSO-d_6) 8.86 (s, 1H), 8.77 (d, J = 8.2 Hz, 1H), 8.55-8.44 (m, 2H), 7.95 (s, 1H), 7.57 (d, J = 7.2 Hz, 1H), 7.41 (d, J = 13.3 Hz, 1H), 7.34-7.20 (m, 3H), 3.99 (s, 3H), 2.30 (s, 3H). MS (ESI) m/z 394.2 $[M+H]^+$.*

4.1.3 ***N'-(2-(dimethylamino)ethyl)-5-methoxy-N'-methyl-N-(4-(3-methyl-1H-indol-1-yl)pyrimidin -2-yl)-2-nitrobenzene-1,4-diamine (20)***

*N,N,N'-trimethylethane-1,2-diamine (2.86 g, 27.96 mmol) was added to a suspension of N-(4-fluoro-2-methoxy-5-nitrophenyl)-4-(3-methyl-1H-indol-1-yl)pyrimidin-2-amine (***19***) (10.00 g, 25.42 mmol), DIPEA (4.91 g, 38.13 mmol) and N,N-dimethyl acetamide (DMAC) (30 mL) in sealed tube. The mixture was heated at 140 °C for 6 h. After being cooled to room temperature, the reaction mixture was added to ice water (60 mL). The precipitate was filtered, and the filtered cake was rinsed with additional cooled MeOH (20 mL) and dried in a vacuum oven to give a red solid (9.60 g, 79.4% yield), which was used without further purification.*

4.1.4 *N1-(2-(dimethylamino)ethyl)-5-methoxy-N1-methyl-N4-(4-(3-methyl-1H-indol-1-yl) pyrimidin-2-yl) benzene-1,2,4-triamine (21)*

*N -(2-(dimethylamino)ethyl)-5-methoxy-N -methyl-N-(4-(3-methyl-1H-indol-1-yl) pyrimidin-2-yl)-2-nitrobenzene-1,4-diamine (***20***) (5.00 g, 10.52 mmol) and Pd/C (10% by weight) (230 mg, 2.10 mmol) were suspended in a mixture of MeOH (100 mL) and stirred under a hydrogen atmosphere for 20 h. The reaction mixture was filtered and the filtrate was concentrated in vacuo. The resulting residue was purified by silica gel chromatography (DCM: MeOH: $NH_3 \cdot H_2O$=20:1:0.1) to afford the title compound (3.50 g, 74.7% yield) : ^{1}H NMR (400 MHz, DMSO-d_6) 8.54 (s, 1H), 8.39 (s, 1H), 8.34 (d, J = 5.7 Hz, 1H), 7.84 (s, 1H), 7.55-7.49 (m, 1H), 7.24-7.11 (m, 3H), 6.99 (d, J = 5.7 Hz, 1H), 6.79 (s, 1H), 3.70 (s, 3H), 2.93 (t, J = 6.6 Hz, 2H), 2.67 (s, 3H), 2.39 (t, J = 6.6 Hz, 2H), 2.28 (s, 3H), 2.17 (s, 6H). MS (ESI) m/z 446.2 $[M+H]^+$.*

4.1.5 *N-(2-((2-(dimethylamino)ethyl)(methyl)amino)-4-methoxy-5-((4-(3-methyl-1H-indol-1-yl)pyrimidin-2-yl)amino)phenyl)acrylamide (6)*

*Acryloyl chloride (710 mg, 7.85 mmol) in DCM (5 mL) was added dropwise to a stirred solution of N1-(2-(dimethylamino)ethyl)-5-methoxy-N1-methyl-N4-(4-(3-methyl-1H-indol-1-yl)pyrimidi n-2-yl)benzene-1,2,4-triamine (***21***) (3.50 g, 7.85 mmol) and DIPEA (2.03 g, 15.70 mmol) in DCM (30 mL) at -10 °C. The resulting solution was maintained at -10 °C for 1 h and then washed with brine, dried over Na_2SO_4, and concentrated. The resulting residue was purified by silica gel chromatography (DCM: MeOH: $NH_3 \cdot H_2O$=40:1:0.1) to afford N-(2-((2-(dimethylamino)ethyl) (methyl)amino)-4-methoxy-5-((4-(3-methyl-1H-indol-1-yl)pyrimidin-2-yl)amino)phenyl)acryl-amide (***6***) (1.50 g, 38.2% yield) as a light yellow solid. ^{1}H NMR (400 MHz, DMSO-d_6) 10.14 (s, 1H), 8.63 (s, 1H), 8.54 (s, 1H), 8.37 (s, 1H), 8.35 (s, 1H), 7.99 (s, 1H), 7.53 (d, J = 7.5 Hz, 1H), 7.20-7.07 (m, 2H), 7.06 (d, J = 5.3 Hz, 2H), 6.41 (dd, J = 16.9,*

10.1 Hz, 1H), 6.22 (dd, J = 16.9, 2.0 Hz, 1H), 5.74 (dd, J = 10.1, 1.9 Hz, 1H), 3.79 (s, 3H), 2.91 (t, J = 5.6 Hz, 2H), 2.75 (s, 3H), 2.34 (t, J = 5.6 Hz, 2H), 2.29 (s, 3H), 2.22 (s, 6H). ^{13}*C NMR (100 MHz, DMSO-*d_6*) 162.39, 160.70, 159.25, 158.05, 148.67, 139.74, 134.79, 132.15, 131.18, 127.35, 126.02, 124.10, 123.28, 122.90, 121.54, 118.66, 117.31, 115.95, 115.67, 105.59, 98.79, 56.86, 55.74, 45.19, 42.22, 9.28. MS (ESI) m/z 500.3* $[M+H]^+$*. HRMS calcd for* $C_{28}H_{34}N_7O_2$ $[M+H]^+$ *500.2769, found 500.2761.*

4.1.6 ***1-(2-chloropyrimidin-4-yl)-5,6-dihydro-4H-pyrrolo[3,2,1-ij]quinolone (18c)***

A suspension of 2,4-dichloropyrimidine (11.37 g, 76.33 mmol) and aluminum chloride (10.18 g, 76.33 mmol) in DME (100 mL) was stirred at ambient temperature for 20 min. To this was added 2,3-dihydro-1H-pyrrolo[3,2,1-ij]quinoline (10.00 g, 63.61 mmol) and the mixture was heated to 80 °C for 6 h. The cooled reaction mixture was added to stirring water (100 mL) and the mixture was stirred for 2 h, filtered and the solid was washed with EtOH (40 mL). The crude product was dried in a vacuum oven to give a red solid (15.46 g, 90.1% yield): ^{1}*H NMR (400 MHz, DMSO-*d_6*) 8.50 (d, J = 5.5 Hz, 1H), 8.45 (s, 1H), 8.09 (d, J = 7.9 Hz, 1H), 7.80 (d, J = 5.5 Hz, 1H), 7.21-7.11 (m, 1H), 7.01 (d, J = 7.1 Hz, 1H), 4.33-4.18 (m, 2H), 2.96 (t, J = 5.9 Hz, 2H), 2.20-2.11 (m, 2H). MS (ESI) m/z 270.2* $[M+H]^+$.

4.1.7 ***3-(6-chloropyrimidin-4-yl)-1-methyl-1H-indole (2a)***

General procedure for the synthesis of **2a** *and* **2b**. *A suspension of 4,6-dichloro-pyrimidine (5.70 g, 38.16 mmol) and aluminum chloride (5.10 g, 38.16 mmol) in DME (60 mL) was stirred at ambient temperature for 10 min. To this was added 1-methyl-1H-indole (5.00 g, 38.16 mmol) and the mixture was stirred at reflux overnight. The cooled reaction mixture was added to stirring water (100 mL) and the mixture was stirred for 1 h, filtered and the solid was washed with EtOH (20 mL). The crude product was dried in a vacuum oven to give a red solid (4.30 g,*

46.2% yield): ^{1}H NMR (400 MHz, DMSO-d_6) 8.92 (s, 1H), 8.58-8.44 (m, 2H), 7.98 (s, 1H), 7.56 (d, J = 8.0 Hz, 1H), 7.33-7.23 (m, 2H), 3.88 (s, 3H). MS (ESI) m/z 244.2 $[M+H]^+$.

4.2. Biological assay

4.2.1 Kinase inhibition assay.

IC_{50} determinations for EGFR and its mutants (Invitrogen) were performed with the HTRF (Homogenous Time-Resolved Fluorescence) KinEASE-TK assay from Cisbio according to the manufacturer's instructions. A typical enzyme reaction contained 0.04 ng/ L wild-type EGFR or 0.02 ng/ L EGFR (T790M/L858R), 0.5 M TK-substrate-biotin, 10 M ATP, 1 mM DTT, 1 mM $MnCl_2$ and 5 mM $MgCl_2$. Compounds were screened at serial diluted concentration in the presence of 1% DMSO with a 15 min pre-incubation of kinase and compounds. All reactions were started by the addition of ATP and TK-substrate-biotin, incubated at room temperature for 60 min and quenched with the stop buffer containing 62.5 nM Strep-XL665 and TK Ab-Cryptate. The plates were incubated for 1 h before being read on ClARIOstar Microplate Reader (BMG LABTECH) using standard HTRF settings. And IC_{50} values were determined using the GraphPad Prism 5.0 software. Each reaction was performed in duplicate, and at least three independent determinations of each IC_{50} were made.

4.2.2 Cellular phosphorylation assay.

A431 (epidermoid carcinoma, EGFR wild type), HCC827 (NSCLC, EGFR delE746-A750) and NCI-H1975 (NSCLC, EGFR L858R/T790M) cells were obtained from the Cell Bank of the Chinese Academy of Sciences (Shanghai, China). A431 cell was maintained in EMEM medium supplemented with 10% FBS (Gibco). HCC827 and NCI-H1975 cells were separately maintained in RPMI-1640 medium supplemented with 10% FBS (Gibco). Assays to measure cellular phosphorylation of endogenous p-EGFR in cell lysates were carried out according to the protocol described in the Pan phospho-EGFR Cellular Assay Kit (Cisbio, no. 64HR1PEG).

Cells were plated (50000 cells/well) in a volume of 100 L of complete media in 96-well cell culture plates and cultured at 37 °C with 5% CO_2 overnight. Inhibitors were solubilized in DMSO and tested in duplicate utilizing 4-fold serial dilutions with the highest concentration at 10 M. Inhibitors were incubated with cells for 2 h at 37 °C with 5% CO_2. For EGFR wild type assays, cells were stimulated for 10 min with EGFR (100 ng/well) before lysis. For all cells post inhibitor treatment (+/- EGF), media was removed and 25 L of 1× lysis buffer was added to each well. Plates were shaken (10 min, 25 °C) to lyse the cells and 12 L of lysate was transferred to the Greiner black 384-well plates. The detection antibody (Anti-phospho EGFR-d2 and Anti-EGFR-Tb) was added to the lysate (3 L/well) and incubated for 1 h at 25 °C. The HTRF signal was measured with ClARIOstar Microplate Reader (BMG LABTECH). And IC_{50} values were determined using the GraphPad Prism 5.0 software.

4.2.3 Determination of pharmacokinetic parameters in rats.

Male Sprague-Dawley rats (200-240 g) were administrated with the test compounds intravenously (iv) at 1 mg/kg and by oral gavage (po) at 10 mg/kg. The compounds **8** *and* **AZD9291** *were dissolved in 2% DMSO, 20% PEG400, and 78% buffered saline for intravenous tail-vein administration or a mixture of 0.5% methylcellulose for oral administration. Blood samples (0.2 mL) were then obtained via orbital sinus puncture at 2 min, 5 min, 15 min, 30 min, 1 h, 2 h, 4 h, 8 h, 12 h and 24 h time points and collected into heparinized tubes. Heparinized blood samples collected for PK analyses were centrifuged at 3500 rpm for 10 min at 25 °C. LC/MS/MS analysis of* **8** *and* **AZD9291** *was performed under optimized conditions to obtain the best sensitivity and selectivity of the analyte in selected reaction monitoring mode (SRM). Plasma concentration-time data were analyzed by a non-compartment model using the software WinNonlin Enterprise, version 6.3 (Pharsight Co., Mountain View, CA).*

4.2.4 Mouse tumor xenograft efficacy study.

H1975 NSCLC xenograft model was established by 5 × 10^6 cells subcutaneously inoculated in C.B-17 SCID mice. Upon attaining an average tumor volume of 100-150 mm^3, animals were randomized into treatment groups (n =9). Each group was dosed by intragastric administration (ig) for 18 days with compound **8** *(5, 10 and 20 mg/kg) daily. The doses were 0.1 mL/10 g of the animal body weight. The size of tumors was measured twice per week with microcalipers. Tumor volume (TV) was calculated as: V = (length × width^2)/2. The individual relative tumor volume (RTV) was calculated as follows: RTV = V_t/V_0, where V_t is the volume on each day of measurement and V_0 is the volume on the day of initial treatment. Therapeutic effect of compound was expressed in terms of T/C% and the calculation formula is T/C (%) = mean RTV of the treated group/mean RTV of the control group × 100%. Tumor growth inhibition (TGI) was calculated using the following formula: TGI = ($TW_{control}$-$TW_{treatment}$) / $TW_{control}$ × 100%, where TW is the mean of tumor weight.*

4.2.5 Computational modeling methods.

LigPrep (v2.2) module in the Schrodinger molecular modeling suite was used for ligand preparation, which produced low energy conformations of ligand using OPLS 2005 force field. The bond orders of these ligands were fixed and the ligands 'cleaned' through LigPrep specifying a pH value of 7.0. The crystal structure of the T790M EGFR kinase (PDB code: 3IKA, http://www.pdb.org/) was selected as the protein target. The docking simulation was performed with Covalent Docking (Schrödinger) using protein models based on in-house crystal structures where Cys797 was bonded to the -carbon of Michael acceptor of molecules [34].

Acknowledgments

This work was supported by the following grants: the National Natural Science Foundation of China (21302097), Natural Science Fund for Colleges and Universities in Jiangsu Province (14KJD350002), Technology Support Program of Science and Technology Department of

Jiangsu Province (BE2014720), National and Local Joint Engineering Research Center of Biomedical Functional Materials and Priority Academic Program Development of Jiangsu Higher Education Institutions (PAPD). We acknowledge the China Pharmaceutical University to provide Schrodinger Suites for molecular docking.

Supporting information.

Detailed procedures for the synthesis of **AZD9291**; Spectral data and NMR spectrum for all target compounds (**7-16, 22-30**); HPLC analysis data for all final compounds; and kinase selectivity data for compound **8**.

Abbreviations used.

EGFR, epidermal growth factor receptor; NSCLC, non-small cell lung cancer; WT, wild type; TL, T790M/L858R; *IC_{50}, half-maximum inhibitory concentration; AUC, area under the curve; $T_{1/2}$, half-time; DCM, dichloromethane; DMAC, N,N-dimethylacetamide; DMF, N,N-dimethyl-formamide; DME, 1,2-dimethoxyethane; DIPEA, N,N-diisopropylethylamine; DMSO, dimethyl sulfoxide; SAR, structure-activity relationship; SD, Sprague-Dawley; UPLC, ultra performance liquid chromatography.*

References

[1] N. E. Hynes; H. A. Lane. ErbB receptors and cancer: the complexity of targeted inhibitors. Nat. Rev. Cancer 2005, 5, 341-354.

[2] M. A. Olayioye; R. M. Neve; H. A. Lane; N. E. Hynes. The ErbB signaling network: receptor heterodimerization in development and cancer. EMBO J. 2000, 19, 3159-3167.

[3] A. Citri; Y. Yarden. EGF-ERBB signaling: towards the systems level. Nat. Rev. Mol. Cell. Biol. 2006, 7, 505-516.

[4] M. L. Barbosa; L. M. Lima; R. Tesch.; C. R. Sant'Anna; F. Totzke; M. G. Kubbutat; G. Schächtele; S. A. Laufer; E. J. Barreiro. Novel 2-chloro-4-anilino- quinazoline derivatives as EGFR and VEGFR-2 dual inhibitors. Eur. J. Med. Chem. 2014, 71, 1-14.

[5] P. M. Ellis; M. Morzycki; B. Melosky; C. Butts; V. Hirsh; F. Krasnoshtein; N. Murray; F. A. Shepherd; D. Soulieres; M. S. Tsao; G. Goss. The role of the epidermal growth factor receptor tyrosine kinase inhibitors as therapy for advanced, metastatic, and recurrent non-small-cell lung cancer: a Canadian national consensus statement. Curr. Oncol. 2009, 16, 27-48.

[6] R. Rosell; T. Moran; C. Queralt; R. Porta; F. Cardenal; C. Camps; M. Majem; G. Lopez-Vivanco; D. Isla; M. Provencio; A. Insa; B. Massuti; J. L. Gonzalez-Larriba; L. Paz-Ares; I. Bover; R. Garcia-Campelo; M. A. Moreno; S. Catot; C. Rolfo; N, Reguart; R. Palmero; J. M. Sanchez; R. Bastus; C. Mayo; J. Bertran-Alamillo; M. A. Molina; J. J. Sanchez; M. Taron, Spanish Lung Cancer Group. Screening for epidermal growth factor receptor mutations in lung cancer. N. Engl. J. Med. 2009, 361, 958-967.

[7] S. Suzuki; Y. Dobashi; H. Sakurai; K. Nishikawa; M. Hanawa; A. Ooi. Protein overexpression and gene amplification of epidermal growth factor receptor in non-small cell lung carcinomas. An immunohistochemical and fluorescence in situ hybridization study. Cancer 2005, 103, 1265-1273.

[8] H. Q. Zhang; F. H. Gong; J. Q. Ye; C. Zhang; X. H. Yue; C. G. Li; Y. G. Xu; L. P. Sun. Design and discovery of 4-anilinoquinazoline-urea derivatives as dual TK inhibitors of EGFR and VEGFR-2. Eur. J. Med. Chem. 2017, 125, 245-254.

[9] J. Han; S. Henriksen; K. G. Nørsett; E. Sundby; B. H. Hoff. Balancing potency, metabolic stability and permeability in pyrrolopyrimidine-based EGFR inhibitors. Eur. J. Med. Chem. 2016, 124, 583-607.

[10] K. M. Amin; F. F. Barsoum; F. M. Awadallah; N. E. Mohamed. Identification of new potent phthalazine derivatives with VEGFR-2 and EGFR kinase inhibitory activity. Eur. J. Med. Chem. 2016, 123, 191-201.

[11] S. Y. Yin; C. M. Tang; B. Wang; Y. Zhang; L. L. Zhou; L. J. Xue; C. Zhang. Design, synthesis and biological evaluation of novel EGFR/HER2 dual inhibitors bearing an oxazolo[4,5-g] quinazolin-2(1H)-one scaffold. Eur. J. Med. Chem. 2016, 120, 26-36.

[12] S. Tracy; T. Mukohara; M. Hansen; M. Meyerson; B. E. Johnson; P. A. Janne. Gefitinib induces apoptosis in the EGFRL858R non-small-cell lung cancer cell line H3255. Cancer Res. 2004, 64, 7241-7244.

[13] S. V. Sharma; D. W. Bell; J. Settleman; D. A. Haber. Epidermal growth factor receptor mutations in lung cancer. Nat. Rev. Cancer 2007, 7, 169-181.

[14] K. Ohashi; Y. E. Maruvka; F. Michor; W. Pao. Epidermal growth factor receptor tyrosine kinase inhibitor-resistant disease. J. Clin. Oncol. 2013, 31, 1070-1080.

[15] C. R. Chong; P. A. Jänne. The quest to overcome resistance to EGFR-targeted therapies in cancer. Nat. Med. 2013, 19, 1389-1400.

[16] S. Kobayashi; T. J. Boggon; T. Dayaram; P. A. Jänne; O. Kocher; M. Meyerson; B. E. Johnson; M. J. Eck; D. G. Tenen; B. Halmos. EGFR mutation and resistance of non-small-cell lung cancer to gefitinib. N. Engl. J. Med. 2005, 352, 786-792.

[17] E. L. Kwak; R. Sordella; D. W. Bell; N. Godin-Heymann; R. A. Okimoto; B. W. Brannigan; P. L. Harris; D. R. Driscoll; P. Fidias; T. J. Lynch; S. K. Rabindran; J. P. McGinnis; A. Wissner; S. V. Sharma; K. J. Isselbacher; J. Settleman; D. A. Haber. Irreversible inhibitors of the EGF receptor may circumvent acquired resistance to gefitinib. Proc. Natl. Acad. Sci. USA. 2005, 102, 7665-7670.

[18] J. A. Engelman; K. Zejnullahu; C. M. Gale; E. Lifshits; A. J. Gonzales; T. Shimamura; F. Zhao; P. W. Vincent; G. N. Naumov; J. E. Bradner; I. W. Althaus; L. Gandhi; G. I. Shapiro; J. M. Nelson; J. V. Heymach; M. Meyerson; K. K. Wong; P. A. Jänne. PF00299804, an irreversible pan-ERBB inhibitor, is effective in lung cancer models with EGFR and ERBB2 mutations that are resistant to gefitinib. Cancer Res. 2007, 67, 11924-11932.

[19] D. Li; L. Ambrogio; T. Shimamura; S. Kubo; M. Takahashi; L. R. Chirieac; R. F. Padera; G. I. Shapiro; A. Baum; F. Himmelsbach; W. J. Rettig; M. Meyerson; F. Solca; H. Greulich; K. K. Wong. BIBW2992, an irreversible EGFR/HER2 inhibitor highly effective in preclinical lung cancer models. Oncogene 2008, 27, 4702-4711.

[20] L. V. Sequist; B. Besse; T. J. Lynch; V. A. Miller; K. K. Wong; B. Gitlitz; K. Eaton; C. Zacharchuk; A. Freyman; C. Powell; R. Ananthakrishnan; S. Quinn; J. C. Soria. Neratinib, an irreversible Pan-ErbB receptor tyrosine kinase inhibitor: results of a Phase II trial in patients with advanced non-small-cell lung cancer. J. Clin. Oncol. 2010, 28, 3076-3083.

[21] L. V. Sequist; J. C. Soria; J. W. Goldman; H. A. Wakelee; S. M. Gadgeel; A. Varga; V. Papadimitrakopoulou; B. J. Solomon; G. R. Oxnard; R. Dziadziuszko; D. L. Aisner; R. C. Doebele; C. Galasso; E. B. Garon; R. S. Heist; J. Logan; J. W. Neal; M. A. Mendenhall; S. Nichols; Z. Piotrowska; A. J. Wozniak; M. Raponi; C. A. Karlovich; S. Jaw-Tsai; J. Isaacson; D.

Despain; S. L. Matheny; L. Rolfe; A. R. Allen; D. R. Camidge. Rociletinib in EGFR mutated non-small-cell lung cancer. N. Engl. J. Med. 2015, 372, 1700-1709.

[22] D. A. Cross; S. E. Ashton; S. Ghiorghiu; C. Eberlein; C. A. Nebhan; P. J. Spitzler; J. P. Orme; M. R. Finlay; R. A. Ward; M. J. Mellor; G. Hughes; A. Rahi; V. N. Jacobs; M. R. Brewer; E. Ichihara; J. Sun; H, Jin; P. Ballard; K. Al-Kadhimi; R. Rowlinson; T. Klinowska; G. H. Richmond; M. Cantarini; D. W. Kim; M. R. Ranson; W. Pao. AZD9291, an irreversible EGFR TKI, overcomes T790M-mediated resistance to EGFR inhibitors in lung cancer. Cancer Discov. 2014, 4, 1046-1061.

[23] H. M. Cheng; S. K. Nair; B. W. Murray; C. Almaden; S. Bailey; S. Baxi; D. Behenna; S. ChoSchultz; D. Dalvie; D. M. Dinh; M. P. Edwards; J. L. Feng; R. A. Ferre; K. S. Gajiwala; M. D. Hemkens; A. J. Fisher; M. Jalaie; T. O. Johnson; R. S. Kania; S. Kephart; J. Lafontaine; B. Lunney; K. K. C. Liu; Z. Y. Liu; J. Matthews; A. Nagata; S. Niessen; M. A.Ornelas; S. T. M. Orr; M. Pairish; S. Planken; S. J. Ren; D. Richter; K. Ryan; N, Sach; H. Shen; T. Smeal; J. Solowiej; S. Sutton; K. Tran; E. Tseng; W. Vernier; M. Walls; S. W. Wang; S. L. Weinrich; S. B. Xin; H. W. Xu; M. J. Yin; M. Zientek.; R. Zhou; J. C. Kath. Discovery of 1-{(3R,4R)-3-[({5-Chloro-2-[(1-methyl-1H-pyrazol-4-yl)amino]-7H-pyrrolo[2,3-d]pyrimidin-4-yl}oxy)methyl]-4-methoxypyrrolidin-1-yl}prop-2-en-1-one (PF-06459988), a potent, WT sparing, irreversible inhibitor of T790M-containing EGFR mutants. J. Med. Chem. 2016, 59, 2005-2024.

[24] P. A. Jänne; J. C. Yang; D. W. Kim; D. Planchard; Y. Ohe; S. S. Ramalingam; M. J. Ahn; S. W. Kim; W. C. Su; L. Horn; D. Haggstrom; E. Felip; J. H. Kim; P. Frewer; M. Cantarini; K. H. Brown; P. A. Dickinson; S. Ghiorghiu; M. Ranson. AZD9291 in EGFR inhibitor-resistant non-small-cell lung cancer. N. Engl. J. Med. 2015, 372, 1689-1699.

[25] P. A. Jänne; S. S. Ramalingam; J. C. H. Yang; M. J. Ahn; D. W. Kim; S. W. Kim; D. Planchard; Y. Ohe; E. Felip; C. Watkins; M. Cantarini; S. Ghiorghiu; M. Ranson. Clinical activity of the mutant-selective EGFR inhibitor AZD9291 in patients (pts) with EGFR inhibitor-resistant non-small cell lung cancer (NSCLC). Clin. Oncol. 2014, 32, 5s.

[26] X. Gao; X. Le; D. B. Costa. The safety and efficacy of osimertinib for the treatment of EGFR T790M mutation positive non-small-cell lung cancer. Expert Rev. Anticancer Ther. 2016, 16, 383-390.

[27] Y. Yosaatmadja; S. Silvab; J. M. Dicksona; A. V. Pattersonb; J. B. Smaillb; J. U. Flanaganb; M. J. McKeagеb; C. J. Squirea. Binding mode of the breakthrough inhibitor AZD9291 to epidermal growth factor receptor revealed. J. Struct. Biol. 2015, 192, 539-544.

[28] R. Heald; K. K. Bowman; M. C. Bryan; D. Burdick; B. Chan; E. Chan; Y. Chen; S. Clausen; B. Dominguez-Fernandez; C. Eigenbrot; R. Elliott; E. J. Hanan; P. Jackson; J. Knight; H. La; M. Lainchbury; S. Malek; S. Mann; M. Merchant; K. Mortara; H. Purkey; G. Schaefer; S. Schmidt; E. Seward; S. Sideris; L. L. Shao; S. M. Wang; K. Yeap; I. Yen; C. Yu; T. P. Heffron. Noncovalent mutant selective epidermal growth factor receptor inhibitors: a lead optimization case history. J. Med. Chem. 2015, 58, 8877-8895.

[29] E. A. Jare-Erijma; T. M. Jov. FRET imaging. Nat. Biotechnol. 2003, 21, 1387-1395.

[30] R. S. Obach. Prediction of human clearance of twenty-nine drugs from hepatic microsomal intrinsic clearance data: an examination of in vitro half-life approach and nonspecific binding to microsomes. Drug Metab. Dispos. 1999, 27, 1350-1359.

[31] P. Baranczewski; A. Stanczak; K. Sundberg; R. Svensson; A. Wallin; J. Jansson; P. Garberg; H. Postlind. Introduction to in vitro estimation of metabolic stability and drug interactions of new chemical entities in drug discovery and development. Pharmacol. Rep. 2006, 58, 453-472.

[32] M. C. Sanguinetti; M. Tristani-Firouzi. hERG potassium channels and cardiac arrhythmia. Nature 2006, 440, 463-469.

[33] X. Cao; T. Lee; M. Holmqvist; D. Mikhailov; Y. Ni; H. Zhang; C. Hogan; M. E. Digan; L. Urban; G. Erdemli. Cardiac ion channel safety profiling on the IonWorks Quattro system. J. Pharmacol. Toxicol. Methods 2011, 64, e8.

[34] K. Zhu; K. W. Bonelli; J. R. Greenwood; T. Day; R. Abel; R. S. Farid; D. Harder. Docking covalent inhibitors: a parameter free approach to pose prediction and scoring. J. Chem. Inf. Model. 2014, 54, 1932-1940.

Captions

Fig. 1. *Structures of different generation EGFR inhibitors*

Fig. 2. Docking pose of **AZD9291** in the complex of EGFR T790M mutant

Fig. 3. Interaction map of **AZD9291** with the EGFR T790M mutant and the overview in the binding site

Fig. 4. Design strategy of the new compounds based on **AZD9291**

Fig. 5. *In vivo activity of* **8** *in the human NSCLC (H1975) xenograft nude mouse model*

Fig. 6. *hERG current inhibition of compounds* **8** *and* **AZD9291**

Scheme 1. *Synthetic Route for Target Compounds* **6-12**

Scheme 2. *Synthetic Route for Target Compounds* **13-16** *and* **22-30**

Table 1. *Enzymatic Inhibitory Activities of Compounds* **6-16** *and* **AZD9291**

Table 2. *Enzymatic Inhibitory Activities of* **22-30** *and* **AZD9291**

Table 3. *Cell Viabilities of Representative Compounds*

Table 4. *Stabilities of Compounds* **8** *and* **AZD9291** *in Liver Microsomes of Various Species*

Table 5. *Stabilities of Compounds* **8** *and* **AZD9291** *in Hepatocyte*

Table 6. *In Vivo Pharmacokinetic Parameters for Compounds* **8** *and* **AZD9291**

Table 7. *In Vivo Antitumor Effect of* **8** *in Human H1975 Xenograft Nude Mouse Model*

- *A novel series of selective covalent EGFR T790M inhibitors were designed and synthesized.*
- C*ompound* **8** effectively *inhibited the enzymatic function of EGFR T790M/L858R and NSCLC H1975 cell.*
- *Compound* **8** *significantly inhibited tumor growth in EGFR T790M/L858R-driven human NSCLC xenograft mouse model.*
- *The lower binding affinities of compound* **8** *to the hERG ion channel suggested that compound* **8** *might be less cardiotoxic than* **AZD9291**.